

A study of effective charge density of swollen poly(vinyl alcohol) membrane mixed with poly(styrenesulfonic acid)

Keiichiro Saito, Akihiko Tanioka* and Keizo Miyasaka

Department of Organic and Polymeric Materials, Tokyo Institute of Technology,
Ookayama, Meguro, Tokyo 152, Japan

(Received 21 February 1994)

A study of the effective charge density of a charged membrane composed of poly(vinyl alcohol) and poly(sulfonate) was carried out. The ratio of the effective charge density obtained from the membrane potential to the net charge density from pH titration was shown to be a function of degree of hydration (H). In order to explain the decrement of the ratio cited above as H increased, a model that includes two kinds of ionic fluxes within the membrane was introduced. This model was found to be able to give a qualitative explanation for the behaviour of the effective charge density of a charged membrane.

(Keywords: poly(vinyl alcohol) membrane; effective charge density; modelling)

INTRODUCTION

Charge density is one of the important parameters that dominate the ionic behaviour in a membrane having charged groups. In order to estimate it, several methods are considered. One of them is to carry out a potentiometric titration, and another is by applying the membrane potential data to the Teorell–Meyer–Sievers theory based on Donnan equilibrium and Nernst–Planck equation^{1–3}. The second is generally called the ‘effective charge density’ of a charged membrane, and is one of the major subjects studied intensively by Kobatake *et al.*^{4–10}. The effective charge density would be less than the net one, because of the interaction between fixed charges and ions. In a series of papers by Kobatake *et al.*^{4–10}, quantitative relationships for the interaction (namely the ‘additivity rule’¹¹, which was first found in the representation of activity coefficients on polyelectrolyte solutions) were introduced into the ionic mobilities and activity coefficients in a charged membrane⁵, considering the fixed charges to be distributed homogeneously, both theoretically and experimentally. On the other hand, they are in fact distributed heterogeneously, especially in some kinds of membranes such as biomembranes and the newly developed artificial ion-exchange membrane¹², which is called an ionomer. So an investigation considering the heterogeneous distribution of fixed charges is required.

In this study, the effective charge density was investigated from the viewpoint of membrane structure, namely the distribution of fixed charge groups. Using the degree of hydration as a characteristic parameter of a membrane, the effective charge density was compared with the net charge density in the membrane. Finally, a model that represents the ionic behaviour in a charged membrane was suggested.

EXPERIMENTAL

Samples

Poly(vinyl alcohol) (PVA, $DP = 2000$; Wako Chemical) and poly(sulfonate) (PSS, 0.4 monomer mol l^{-1} ; Asahi Chemical) were used to prepare negatively charged membranes. PVA was saponified before use. PSS was used without further purification.

First, both PVA and PSS were dissolved in water and heated to 100°C and stirred well. Then the solution was cast on a flat poly(methyl methacrylate) plate to dry at 25°C for more than 7 days. The weight ratio of PVA and PSS was 12:1, 6:1, 4:1 and 3:1, respectively. These prepared samples were annealed at 140°C or 180°C under vacuum for about half an hour to make their degree of hydration different by physical crosslinking. Some of them were even soaked in a solution of 0.1 wt% glutaraldehyde, 1 wt% HCl and 20 wt% NaCl for about 24 h in order to decrease their degree of hydration by chemical crosslinking. Finally, samples were soaked in ion-exchanged water to be swollen.

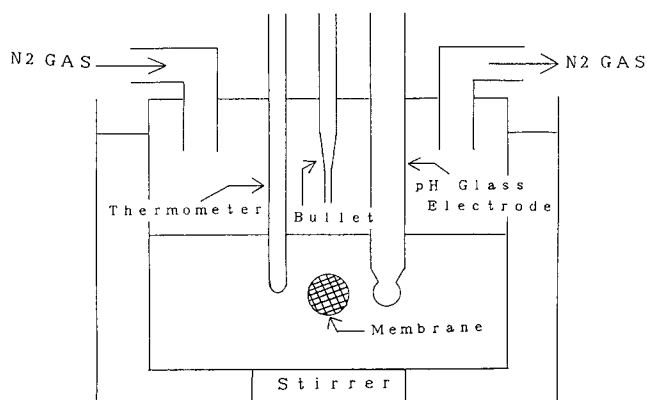
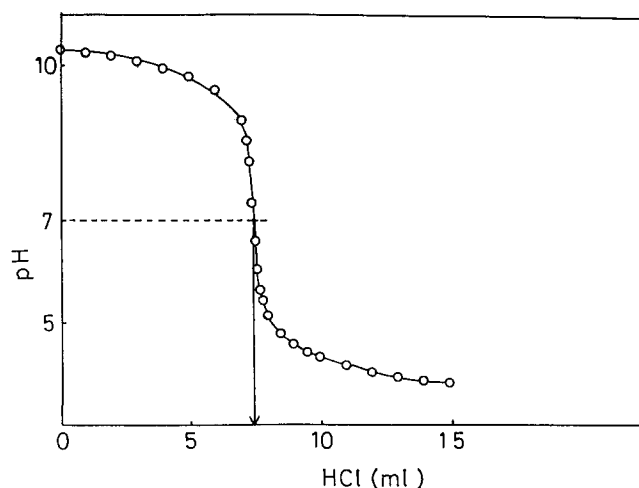
Degree-of-hydration measurements

After soaking the samples in ion-exchanged water for more than 24 h, they were wiped with filter paper and weighed quickly. Degree of hydration was determined according to:

$$H = \frac{\text{water within membrane}}{\text{volume of membrane}} = \frac{(w_w - w_d)/1.0}{(w_d/1.3) + (w_w - w_d)/1.0} \quad (1)$$

where w_w and w_d are swollen and dried membrane weight, and 1.3 and 1.0 are densities of PVA and water.

* To whom correspondence should be addressed


Figure 1 Apparatus for potentiometric (pH) titration of membrane

Figure 2 Typical titration curve of membrane (PSS 14 wt%, annealed at 140°C, concentration of HCl used is $2 \times 10^{-3} \text{ mol l}^{-1}$). The arrow indicates the equivalent point of the titration

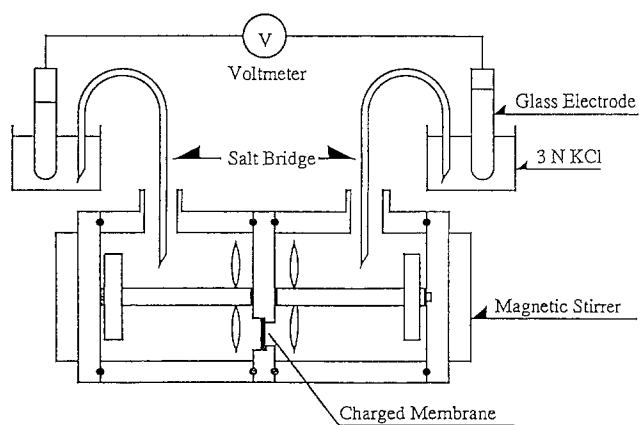
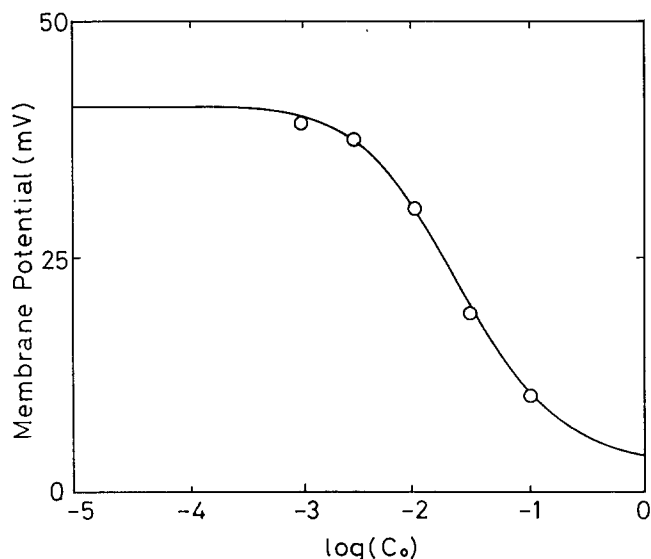
pH titration

The apparatus for pH titration is shown in *Figure 1*. All the procedures that follow were carried out along the lines of the method in ref. 13 and under N_2 gas flow.

First, membranes were soaked in HCl solution (concentration approximately 3 N) for more than 24 h to let all their fixed charges be substituted into acid type. Secondly, membranes were washed with ion-exchanged water to remove any excess HCl that remained in the membrane. After that, they were introduced into 1.0 mol l^{-1} KCl solution and a precise amount of KOH solution (0.1 or 0.01 mol l^{-1}) was used to carry out pH reverse titration with HCl. We obtained the results of titrations as shown in *Figure 2*, from which we could determine the equivalent point and obtain 'the fixed charge density by pH titration' (C_{xt}). For pH measurement, a complex electrode (GST-5211C, TOA Electric) and pH meter (HM-20E, TOA Electric) were used.

Measurement of membrane potential

The apparatus for measurement of membrane potential is shown in *Figure 3*. The concentration ratio of KCl solution in one side to that in the other, which contact right and left side of the membrane, respectively, was always 5 and the measurements were carried out with the concentration of the lower side of 1×10^{-3} , 3×10^{-3} , 1×10^{-2} , 3×10^{-2} , 0.1 and 0.3 mol l^{-1} , respectively. The


Figure 3 Apparatus for measurement of membrane potential

Figure 4 Typical result of membrane potential measurements (PSS 14 wt%, annealed at 140°C). C_0 has the same meaning as in the text

solutions of both sides were stirred by magnetic stirrers to minimize the effect of boundary layer on the potential. An Ag-AgCl electrode (HS-205C, TOA Electric) with KCl salt bridge and the same pH meter as was used in the pH titration were used for measurement of potential difference. Typical results of membrane potential measurements are shown in *Figure 4*. The results were applied to the Teorell-Meyer-Sievers (TMS) equation (equation (2)) and 'the charge density by membrane potential' (C_{xm}) was obtained:

$$\begin{aligned} \Delta\phi &\equiv \Delta\phi_{\text{Don}(0 \rightarrow m)} + \Delta\phi_{\text{diff}} + \Delta\phi_{\text{Don}(m \rightarrow d)} \\ &= -\frac{RT}{F} \ln \left(\frac{C_d [1 + (2C_0/QX)^2]^{1/2} + 1}{C_0 [1 + (2C_d/QX)^2]^{1/2} + 1} \right) \\ &\quad - \frac{RT}{F} W \ln \left(\frac{[1 + (2C_d/QX)^2]^{1/2} + W}{[1 + (2C_0/QX)^2]^{1/2} + W} \right) \quad (2) \end{aligned}$$

where $\Delta\phi_{\text{Don}(0 \rightarrow m)}$ and $\Delta\phi_{\text{Don}(m \rightarrow d)}$ are the Donnan potentials of each side of the membrane, $\Delta\phi_{\text{diff}}$ is the diffusion potential in the membrane, C_0 and C_d are KCl concentrations of the higher and lower sides ($C_0 = 5C_d$),

$$Q \equiv \left(\frac{\gamma_+ \gamma_-}{k_+ k_-} \right)^{1/2} \quad W \equiv \frac{u_+ - u_-}{u_+ + u_-}$$

X is the fixed charge density, γ_i is the activity coefficient

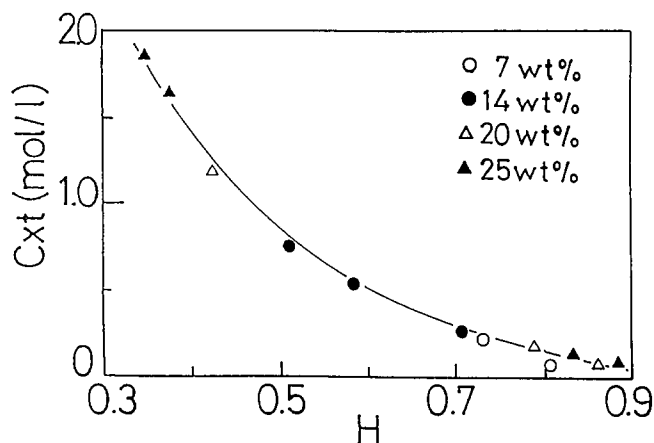


Figure 5 C_{xt} (charge density by pH titration) as a function of degree of hydration (H). Symbols used indicate the weight ratio of PSS to PVA

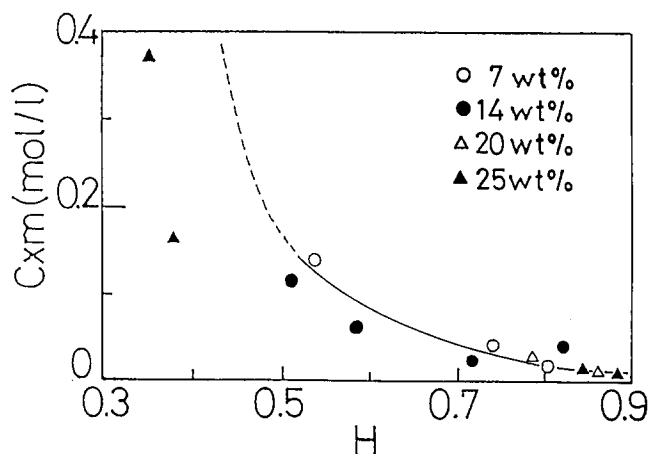


Figure 6 C_{xm} (charge density by membrane potential measurement) as a function of degree of hydration (H). Symbols are the same as in Figure 5

of *i*th ion in the membrane, *k_i* is the distribution coefficient of *i*th ion between the membrane phase and outer solution and *u_i* is the ionic mobility of *i*th ion in the membrane.

RESULTS AND DISCUSSION

C_{xt} values are shown as a function of degree of hydration (H) in Figure 5. C_{xt} seems to be a unique function of degree of hydration of swollen membranes. In Figure 7, logarithmic C_{xt} is plotted as a function of logarithmic H. The good linear relationship is kept through the whole range of H. It means that C_{xt} is a unique function of H and has no relationship with how many charges are fixed, which implies that the hydration phenomenon of a membrane is influenced not only by the characteristics of PVA matrix but also by its fixed charge group. One should note that C_{xt} characterizes net or 'existing' fixed charges and has nothing to do with how they are distributed in the membrane.

We obtained C_{xm} by applying the membrane potential results, typically shown in Figure 4, to the TMS theory (equation (2)). As we could not estimate exact values of activity coefficients and mobilities of ions in the membranes, the following assumptions are required before analysis¹⁰.

Assumption A: $\gamma_i = 1$ (assumption of ideal Donnan equilibrium) and $k_i = 1$, where γ_i and k_i are activity and distribution coefficients of *i*th ion, respectively.

Assumption B: $u_+/u_- = \text{constant}$, where u_i is mobility of *i*th ion in the membrane.

Assumption C: Fixed charge density, which should be constant through a membrane, does not depend on the concentration of the salt solution contacting with each side of a membrane.

Then equation (2) is modified to get:

$$\Delta\phi = -\frac{RT}{F} \ln\left(\frac{C_d [1 + (2C_0/C_{xm})^2]^{1/2} + 1}{C_0 [1 + (2C_d/C_{xm})^2]^{1/2} + 1}\right) - \frac{RT}{F} W \ln\left(\frac{[1 + (2C_d/C_{xm})^2]^{1/2} + W}{[1 + (2C_0/C_{xm})^2]^{1/2} + W}\right) \quad (3)$$

Applying membrane potential data to equation (3), we got C_{xm} as 'a parameter', which is called the 'effective charge density of a charged membrane', by curve fitting. C_{xm} values are shown as a function of degree of hydration (H) in Figure 6. The dependence of C_{xm} on H seems to

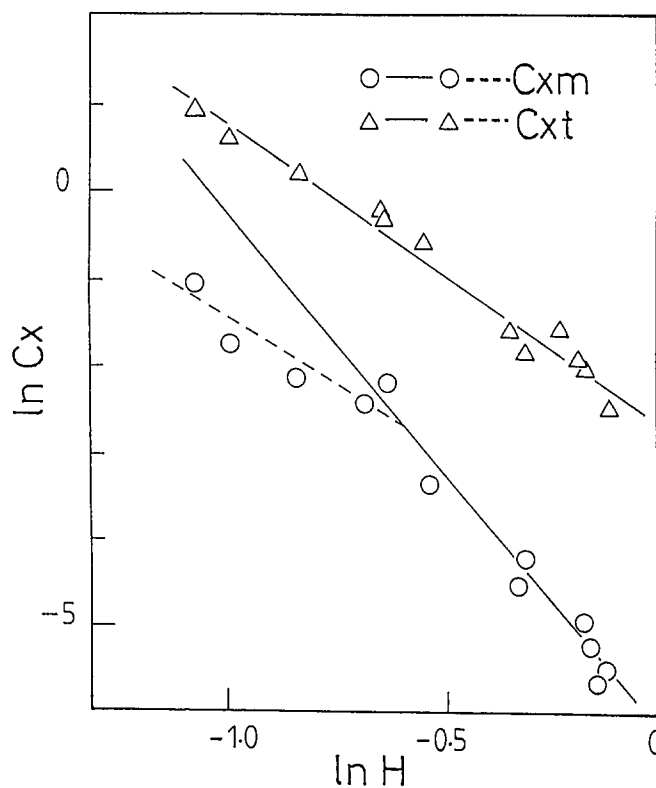


Figure 7 Plots of ln C_{xt} and ln C_{xm} as functions of ln H

have the same tendency as C_{xt}. The logarithmic C_{xm} are shown as a function of logarithmic H in Figure 7. The slope is nearly the same as C_{xt} below ln H = -0.6 and the corresponding value of H is approximately 0.55, and larger than that with ln H > -0.6.

The ratio of C_{xm} to C_{xt}, C_{xm}/C_{xt}, is shown as a function of degree of hydration (H) in Figure 8. According to Figure 8, it is apparent that in the lower H region C_{xm}/C_{xt} is almost 0.2, which is generally obtained for charged membranes such as collodion membranes^{5,7,10}. It decreases and becomes less than 0.1 as H increases.

It should be noted that C_{xm} in equation (3) corresponds to QX in equation (2) and X accords with C_{xt} experimentally. This means that C_{xm}/C_{xt} leads to Q. From a physicochemical point of view, as was cited before, Q

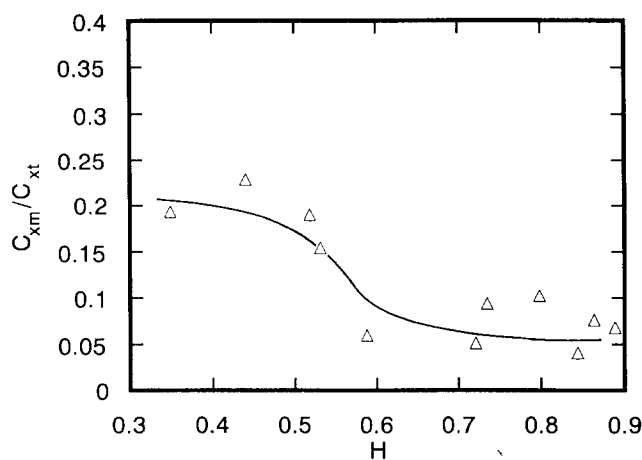


Figure 8 Plot of C_{xm}/C_{xt} as a function of degree of hydration (H)

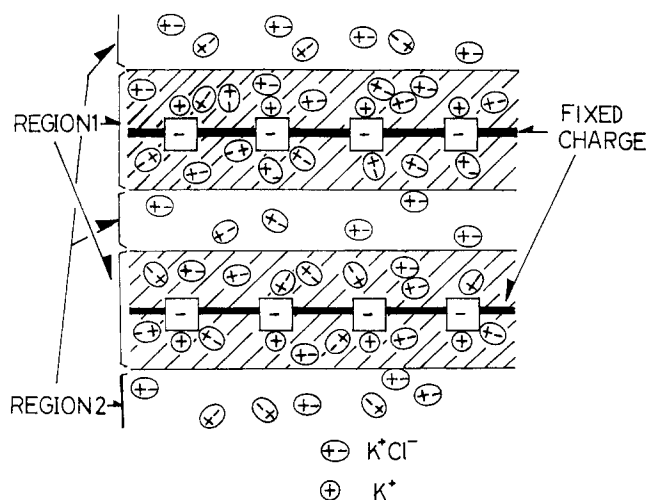


Figure 9 Typical picture of the model considered in this study. Ions existing in a membrane are categorized into two types here. Region 1 is around fixed charge groups, and region 2 is other than that area

is proportional to the square root of the product of cation and anion activity coefficients, $(\gamma_+ \gamma_-)^{1/2}$, and is inversely proportional to the square root of the product of cation and anion distribution coefficients within the membrane, $(k_+ k_-)^{1/2}$. The distribution coefficients of both ions between membrane phase and outer solution could be assumed to be unity, and γ_- in the membrane is also expected to be unity if the activity coefficient of Cl^- is assumed to be the value according to the 'additivity rule'¹¹.

So one of the reasons why C_{xm}/C_{xt} ($=Q$) is a decreasing function of H might be lowering of γ_+ . In polyelectrolyte solution, the extent of attraction of counter-ions by polyions largely influences their activity coefficients. For this reason, the distribution of the counter- and co-ions in the surrounding fixed charge groups should be included when calculating the membrane potential. So counter- and co-ions with the effect of fixed charge groups should be distinguished from those ions without it in a membrane phase. Petropoulos *et al.*¹⁴ showed that 'the non-equipotential volume pore model', which is the modified version of the equipotential volume pore model (EVM) by Vickerstaff¹⁵, gave meaningful interpretation to the distribution behaviour of ions between the charged membrane phase and outer aqueous solution.

Considering the discussion cited above, we construct a type of model that shows the state of ionic flux and derive a membrane potential equation. Within a membrane, we consider counter- and co-ionic flux in the region where fixed charges exert influences (region 1), and also the same flows in the region where they do not (region 2). The fraction of counter- and co-ions that exist in region 1 are α and β , respectively, where $0 < \alpha < 1$ and $0 < \beta < 1$. On the other hand, the fraction of counter- and co-ions that exist in region 2 are $1-\alpha$ and $1-\beta$, respectively. Electrical neutrality is given by equation (4) for region 1 and equation (5) for region 2:

$$\alpha B_m = \beta A_m + X \quad (4)$$

$$(1-\alpha)B_m = (1-\beta)A_m \quad (5)$$

A typical picture of the model that we consider is shown in Figure 9.

First, we consider the Donnan potential, which occurs over the surface of each side of a membrane. The Donnan potential is generated over two phases, one of which has fixed charge groups (unpermeable molecules) and the other has not. We consider three phases, which are region 1 and region 2 in the membrane and the outer solution. The Donnan potential should be studied over each phase, meaning that three patterns of potential differences would be considered. However, the potential difference between region 1 and region 2 is neglected in this study. Chemical potentials of membrane phase and outer solutions are assumed to be equal at the surfaces. For the surface between the membrane phase region 2 and KCl solution of higher-concentration side, equation (6) for counter-ion and equation (7) for co-ion are available:

$$RT \ln C_0 = RT \ln[(1-\alpha)B_m(0)] + F\Delta\phi_{\text{Don}(0 \rightarrow m)} \quad (6)$$

$$RT \ln C_0 = RT \ln[(1-\beta)A_m(0)] - F\Delta\phi_{\text{Don}(0 \rightarrow m)} \quad (7)$$

Over the membrane phase region 1 and KCl solution of higher-concentration side, equation (8) for counter-ion and equation (9) for co-ion are available:

$$\mu_{+0} + RT \ln C_0 = \mu_{+m} + RT \ln[\gamma_+ \alpha B_m(0)] + F\Delta\phi_{\text{Don}(0 \rightarrow m)} \quad (8)$$

$$\mu_{-0} + RT \ln C_0 = \mu_{-m} + RT \ln[\gamma_- \beta A_m(0)] - F\Delta\phi_{\text{Don}(0 \rightarrow m)} \quad (9)$$

Equations for the surface over membrane phase and KCl solution of lower-concentration side can be obtained by replacing C_0 , $B_m(0)$ and $A_m(0)$ by C_d , $B_m(d)$ and $A_m(d)$ in equations (6)–(9), where B_m and A_m are counter- and co-ion in the membrane. The other symbols have their usual meanings.

Therefore the Donnan potential, including both sides, is given by equation (10), which is actually the same as of the original TMS equation:

$$\begin{aligned} \Delta\phi_{\text{Don}} &= \Delta\phi_{\text{Don}(0 \rightarrow m)} + \Delta\phi_{\text{Don}(m \rightarrow d)} \\ &= -\frac{RT}{F} \ln \left(\frac{C_d [1 + (2C_0/QX)^2]^{1/2} + 1}{C_0 [1 + (2C_d/QX)^2]^{1/2} + 1} \right) \quad (10) \end{aligned}$$

Secondly, we consider the diffusion potential. There are two ionic fluxes for one region, one of which is of counter-ions and the other is of co-ions. In total, four ionic fluxes are dealt with in this case. Within region 1, counter- and co-ionic fluxes can be expressed by equations (11) and (12); equations (13) and (14) are for

each flux in region 2:

$$J_+ = -u_+ \alpha B_m \left(RT \frac{d}{dx} \ln(\alpha B_m) + F \frac{d\phi_m}{dx} \right) \quad (11)$$

$$J_- = -u_- \beta A_m \left(RT \frac{d}{dx} \ln(\beta A_m) - F \frac{d\phi_m}{dx} \right) \quad (12)$$

$$J'_+ = -u(1-\alpha)B_m \left(RT \frac{d}{dx} \ln(\alpha B_m) + F \frac{d\phi_m}{dx} \right) \quad (13)$$

$$J''_- = -u(1-\beta)A_m \left(RT \frac{d}{dx} \ln(\beta A_m) - F \frac{d\phi_m}{dx} \right) \quad (14)$$

where u means ionic mobility of K^+ ion in water, which actually is equal to that of Cl^- in water; the x axis is perpendicular to the membrane surface.

Paying attention to the condition of zero electricity in a membrane, which is given by equation (15):

$$J_+ + J'_+ = J_- + J''_- \quad (15)$$

the diffusion potential is shown by equation (16):

$$\Delta\phi_{diff} = \frac{RT}{F} \frac{\alpha\beta(u_- - u_+) + (\alpha - \beta)u}{\alpha\beta(u_+ + u_- - 2u) + (\alpha + \beta)u} \ln \left(\frac{[\alpha\beta(u_+ + u_- - 2u) + (\alpha + \beta)u] \{ [1 + (2C_d/QX)^2]^{1/2} + 1 \} - 2\alpha[\beta u_- + (1 - \beta)u]}{[\alpha\beta(u_+ + u_- - 2u) + (\alpha + \beta)u] \{ [1 + (2C_o/QX)^2]^{1/2} + 1 \} - 2\alpha[\beta u_- + (1 - \beta)u]} \right) \quad (16)$$

The mobility of counter-ions in a charged membrane is assumed to follow equation (17a) by analogy with the 'additivity rule' for the activity coefficient of the counter-ion in polyelectrolyte solution; on the other hand, that of the co-ion is kept constant (equation (17)):

$$u_+ = \frac{C' + QX}{C' + X} u \quad (17a)$$

$$u_- = u \quad (17b)$$

where C' is the mean concentration of salt, which is defined as $C' = (C_o + C_d)/2$.

Thus the diffusion potential of our model is derived using equations (17) as:

$$\Delta\phi_{diff} = \frac{RT}{F} \frac{\alpha\beta[1 - (C' + QX)/(C' + X)] + (\alpha - \beta)}{\alpha\beta[(C' + QX)/(C' + X) - 1] + (\alpha + \beta)} \ln \left(\frac{\{ \alpha\beta[(C' + QX)/(C' + X) - 1] + (\alpha + \beta) \} \{ [1 + (2C_d/QX)^2]^{1/2} + 1 \} - 2\alpha}{\{ \alpha\beta[(C' + QX)/(C' + X) - 1] + (\alpha + \beta) \} \{ [1 + (2C_o/QX)^2]^{1/2} + 1 \} - 2\alpha} \right) \quad (18)$$

Finally, the sum of the Donnan and diffusion potentials makes the membrane potential, and is shown by:

$$\begin{aligned} \Delta\phi &= \Delta\phi_{Don} + \Delta\phi_{diff} \\ &= \frac{RT}{F} \ln \left(\frac{C_d [1 + (2C_o/QX)^2]^{1/2} + 1}{C_o [1 + (2C_d/QX)^2]^{1/2} + 1} \right) \\ &\quad + \frac{RT}{F} \frac{\alpha\beta[1 - (C' + QX)/(C' + X)] + (\alpha - \beta)}{\alpha\beta[(C' + QX)/(C' + X) - 1] + (\alpha + \beta)} \ln \left(\frac{\{ \alpha\beta[(C' + QX)/(C' + X) - 1] + (\alpha + \beta) \} \{ [1 + (2C_d/QX)^2]^{1/2} + 1 \} - 2\alpha}{\{ \alpha\beta[(C' + QX)/(C' + X) - 1] + (\alpha + \beta) \} \{ [1 + (2C_o/QX)^2]^{1/2} + 1 \} - 2\alpha} \right) \end{aligned} \quad (19)$$

Using a computer, the membrane potentials were calculated by equation (19) with varying α and β . Typical results are given in Figure 10. It is generally said that the region where a rapid drop of the potential occurs indicates 'the effective charge density of the system'. Figure 10 shows that 'the region' mentioned above can be varied by changing only α and β , which means 'the effective charge density' should be changed. It turned out that the effective charge density of a membrane should change as a result

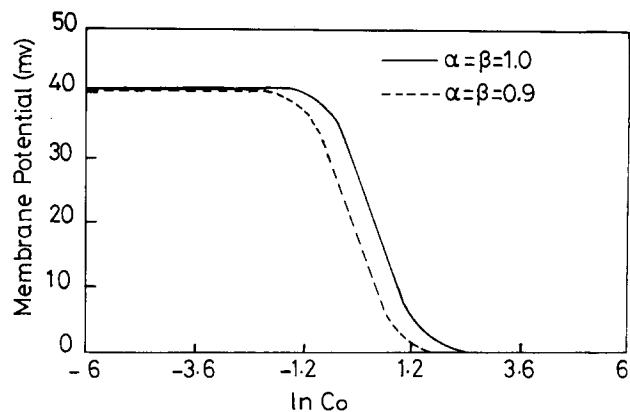


Figure 10 Typical picture of the change of membrane potential curves caused by varying of α and β . Reduction of α and β allows the curve to shift to the left, which means decrement of effective charge density

of the varied ionic atmosphere near a fixed charge group caused by the change of the hydration state of a membrane through the relationship between the reduction of γ_- and the rise of degree of hydration (H).

Though our results should be physically acceptable, some problems are left unresolved. One of those is about the interface between a membrane phase and outer solution. In our system, as previously employed, Donnan potential differences over the interface are assumed to be stepwise, while this assumption is not probable¹⁶⁻¹⁹. A second one is that the potential difference between region 1 and region 2 is neglected within the membrane.

REFERENCES

- 1 Teorell, T. *Prog. Biophys. Biophys. Chem.* 1953, 3, 305
- 2 Meyer, K. H. and Sievers, J. F. *Helv. Chim. Acta* 1936, 19, 649, 665, 987
- 3 Higa, M., Tanioka, A. and Miyasaka, K. *J. Membr. Sci.* 1988, 37, 251
- 4 Yuasa, M., Kobatake, Y. and Fujita, H. *J. Phys. Chem.* 1968, 72, 2871

- 5 Kamo, N., Toyoshima, Y., Nozaki, H. and Kobatake, Y. *Kolloid-Z. Z. Polym.* 1971, **248**, 914
- 6 Kamo, N., Toyoshima, Y. and Kobatake, Y. *Kolloid-Z. Z. Polym.* 1971, **249**, 1061
- 7 Kamo, N. and Kobatake, Y. *Kolloid-Z. Z. Polym.* 1971, **249**, 1069
- 8 Ueda, T., Kamo, N., Ishida, N. and Kobatake, Y. *J. Phys. Chem.* 1972, **76**, 2447
- 9 Kamo, N., Oikawa, M. and Kobatake, Y. *J. Phys. Chem.* 1973, **77**, 92
- 10 Kamo, N. and Kobatake, Y. *Seibutsu-butsuri (Biophysics)* 1971, **11**, 23 (in Japanese)
- 11 Rice, S. and Nagasawa, M. 'Polyelectrolyte Solutions', Academic Press, New York, 1961, p. 399
- 12 Hsu, W. Y. and Berzins, T. *J. Polym. Sci., Polym. Phys. Edn.* 1985, **23**, 933
- 13 Tasaka, M., Aoki, N., Kondo, Y. and Nagasawa, M. *J. Phys. Chem.* 1975, **79**, 1307
- 14 Tsimboukist, D. G. and Petropoulos, J. H. *J. Chem. Soc.* 1979, **75**, 705
- 15 Vickerstaff, T. 'Physical Chemistry of Dyeing', 2nd Edn, Oliver and Boyd, London, 1954, Ch. 7
- 16 Kondo, T., Ohshima, H., Muramatsu, N. and Makino, K. 'Biophysical Chemistry', Sankyo, Tokyo, 1992, Ch. 4 (in Japanese)
- 17 Ohshima, H. and Konto, T. *J. Theor. Biol.* 1987, **128**, 187
- 18 Ohshima, H. and Konto, T. *J. Colloid. Interface Sci.* 1988, **123**, 136
- 19 Ohshima, H. and Konto, T. *J. Colloid Interface Sci.* 1993, **155**, 499